ADVANCED FUNCTIONAL MATERIALS
www.afm-journal.de

Ultra-Flexible Boron-Oxygen 3D Solid-State Networks

Frederik Claeyssens, Judy N. Hart, Nicholas C. Norman, and Neil L. Allan**

The existence of ultra-flexible low-energy forms of boron oxides (B_2O_3 and BO) is demonstrated, in particular structures in which B_3O_3 or B_4O_2 six-membered rings are linked by single B-O-B bridges. The minima in the energy landscapes are remarkably broad; the variation in the internal energies is very small over a very large range of volumes. Such volume changes may even exceed 200%. This remarkable behavior is attributed predominantly to the pronounced angular flexibility of the B-O-B bridges linking the rings, which is unusual for a covalent bond. At larger volumes, the structures are nanoporous; the pores collapse upon compression with negligible change in energy, making these suitable as guest-host materials. In marked contrast, in other materials where low density frameworks have been reported or predicted, such low-density phases are considerably higher in energy. The flexibility of the structures also offers a resolution of the long-standing controversy reconciling the structure and density of vitreous B_2O_3.

1. Introduction

Textbooks use most binary oxides as classic examples of densely-packed systems. A given compound generally adopts only a small number of structures, which correspond to well-defined local, narrow minima in the energy landscape. At given temperature and pressure known stable forms have similar densities. Detailed examination of these and other local minima in energy landscapes[1,2] have often suggested possible alternative phases with higher internal energies, separated by substantial thermodynamic and kinetic barriers from the lowest-energy forms. Familiar routes to such higher (internal) energy structures include high pressure for structures with higher densities.[3] CaO for example transforms from the rocksalt to the CsCl structure at around 60 GPa with a decrease in volume of ≈10%. Reduced dimensionality, such as in various reconstructed and strained nanostructures and thin films, can also alter the energy landscapes dramatically because of the interfacial contributions to the relative energies. A good example is a planar graphene (*h*-BN) form of ZnO, which we predicted[4] and was subsequently confirmed experimentally.[5]

More recently, particular attention has been drawn to possible nanoporous polymorphic phases with densities *lower* rather than higher than the ambient form.[6–8] Ab initio calculations have suggested that new low-density nanoporous crystalline phases of MgO and ZnO for example may be accessible by coalescence of nanocluster building blocks. Postulated polymorphs have unit cell volumes 20–110% larger than those of known structures under ambient conditions, and are similar topologically to known SiO_2 nanoporous crystals. Nanoporous phases of alkali metal halides have also been proposed.[9] These predicted low-density phases are all considerably higher in internal energy than the known structures.

In this paper we demonstrate the existence of ultra-flexible, low-density nanoporous forms of boron oxides. B_2O_3 has received considerable attention[10–12] and very recently[12] the possible high number of low-energy polymorphs has been linked to its ease of vitrification. We begin by noting that a wide range of B-O-B angles is well-established for borate glasses[13] and also theoretically[14] for $H_2B\text{-}O\text{-}BH_2$. We have confirmed there are two distinct minima in the energy landscape for this small molecule—one with D_{2d} symmetry and a B-O-B angle of 180°, the other C_{2v} symmetry and an angle of 125°. The energy difference between the two is only 3 kJ mol^{-1} and the energy barrier between them only twice this. We have investigated this unusual behavior further with calculations on the molecules $(B_4O_2H_3)\text{-}O\text{-}(B_4O_2H_3)$ and $(B_3O_3H_2)\text{-}O\text{-}(B_3O_3H_2)$ (equivalent to two six-membered rings linked by a B-O-B bridge, a possible structural feature in B_2O_3 glasses, **Figure 1**). We then examine the consequences of this flexibility for solid, low-energy polymorphs of B_2O_3 and BO. The results reveal very wide minima in the energy landscapes for particular forms of both compounds. These correspond to stable nanoporous structures, in which the pores can easily be collapsed or expanded, a characteristic at least partly related to the flexibility of B-O-B bonds and not previously recognized.

F. Claeyssens
Materials Science and Engineering Department
Kroto Research Institute
University of Sheffield
Broad Lane, Sheffield, S3 7HQ, UK
E-mail: F.Claeyssens@sheffield.ac.uk
J. N. Hart, N. C. Norman
School of Chemistry
Cantock's Close
University of Bristol
Bristol BS8 1TS, UK
N. L. Allan
School of Chemistry
Cantock's Close
University of Bristol
Bristol BS8 1TS, UK
E-mail: N.L.Allan@bris.ac.uk

DOI: 10.1002/adfm.201300172

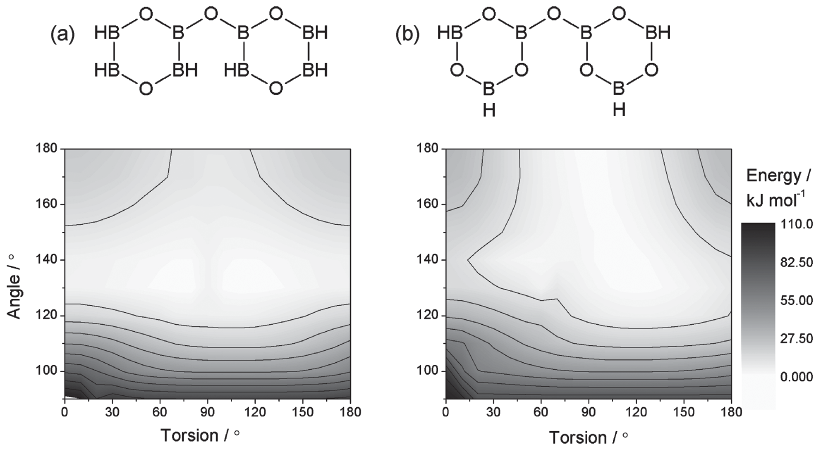

Figure 1. Energies of the molecules a) $(B_4O_2H_3)$-O-$(B_4O_2H_3)$ and b) $(B_3O_3H_2)$-O-$(B_3O_3H_2)$ as a function of B-O-B bridge angle and the B–B..B–B (a) or O-B..B-O (b) torsion angle, calculated using B3LYP as described in the text. Contour heights denote energies in kJ mol^{-1} relative to the global minimum.

2. Results

The variation of energy as a function of the B-O-B bridge angle and the BBBB/OBBO torsion angle in both $(B_4O_2H_3)$-O-$(B_4O_2H_3)$ and $(B_3O_3H_2)$-O-$(B_3O_3H_2)$ is very flat, as is clear from the contour plots in Figure 1. The global minimum energy corresponds to a bridge angle of 140°, considerably smaller than that for H_2B-O-BH_2 (180°).[14] For all three molecules it is clear that there is a wide range both of bridging angles and torsion angles all within a few kJ mol^{-1} of the lowest energy. A simple valence-bond picture can explain this large variation (**Scheme 1**). There are four resonance structures, one with only single bonds and favoring a smaller B-O-B bond angle and three with O=B double bond(s) and favoring a larger angle. Note that this bonding model is only appropriate for molecules containing three-, but not four-, coordinate boron because boron is restricted to an octet of valence electrons.

In molecules, Si-O-Si, Si-O-Al, Al-O-Al and Ge-O-Ge linkages are often also very flexible.[15–17] For example, in H_3 Si-O-SiH_3 and $(HO)_3$Si-O-Si$(OH)_3$, the variation of energy with the Si-O-Si angle is shallow and also typically a few kJ mol^{-1} over the range 130°–180°.[15,16] We have carried out calculations on $(HO)_3$Si-O-Si$(OH)_3$ and $(HO)_2$Al-O-Al$(OH)_2$ at the same level of theory as used for our boron-containing molecules (see the Supporting Information) which confirm this flexibility. Implications for the solid state[18] include a wide range of Si-angles in silicates and correlations between the angle distribution in zeolite frameworks and their relative energy.[19]

Thus the remarkable flexibility we have observed in molecules containing B-O-B bridges connecting two six-membered rings raises the question if and how this flexibility influences solid-state properties and behavior. In this report we explore the effects of replacing B atoms with B_3O_3 rings in a number of B_2O_3 structures. We investigated four different structures A-D with different unit cell sizes (3, 4, 6 and 8 formula units respectively), all built from triangular BO_3 units. An analogous set of structures A-R, B-R, C-R and D-R were formed by replacing all the boron atoms with B_3O_3 rings. It is important to note that the B atom and B_3O_3 rings are interchangeable three-coordinate structural building blocks; the overall stoichiometry is preserved, as shown in the schematic examples in **Figure 2**.

Structure A (shown in the Supporting Information) is the known α-B_2O_3 crystal structure.[20] This structure is related to the planar sheet in Figure 2c. Structure B is taken from ref. [12] (where it is referred to as T2) and is included here to provide a range of different unit cell sizes. Structures A-R (shown in Supporting Information) and B-R are formed by replacing every boron atom in A and B respectively with a B_3O_3 ring.

To construct Structures C-R and D-R, we started from 2D sheets constructed from structural arrangements similar to those observed, for example, in B_3O_3-ring-based networks such as $B_6O_9(en)_2@(H_2en)Cl_2$, $B_6O_9(en)$ and $(H_2en)_2(Hen)_2B_{16}O_{27}$ (Figure 2 and **Figure 3**).[21,22] The 2D sheets contain different numbers of building blocks surrounding the nanopores, and this number is the same whether the blocks are single boron atoms or B_3O_3 rings. The DFT optimized energies of all the 2D sheets differ at most by only 4 kJ mol^{-1}.

The 3D structures (C-R in Figure 3b and D-R in Figure 3d) were generated from these 2D sheets by breaking one intralayer B-O-B bond per unit cell and then forming one interlayer B-O-B bond per unit cell. The analogue structures C and D are formed by the substitution of a boron atom for every B_3O_3 ring.

We present in **Figure 4** energy vs. volume curves for the four structures without B_3O_3 rings, A, B, C and D (Figure 4a), as well as their analogues with the rings, A-R, B-R, C-R and D-R (Figure 4b). The variation of energy with volume for structures A-R, B-R C-R and D-R is remarkably flat, varying by <2 kJ mol^{-1} over an enormous range of volumes (for D-R, as much as 15–65 Å^3 atom^{-1}). This is a variation which to our knowledge is unprecedented and indicates very broad local minima in the energy landscape.

For comparison, we turn briefly to boron oxides with different stoichiometries and in particular to a low-energy form of boron monoxide, a compound which has received recent attention.[23] Following ref. [18], we examine a structure based on sheets consisting of six-membered B_4O_2 rings (rather than

Scheme 1. Possible resonance structures for R_2B-O-BR_2

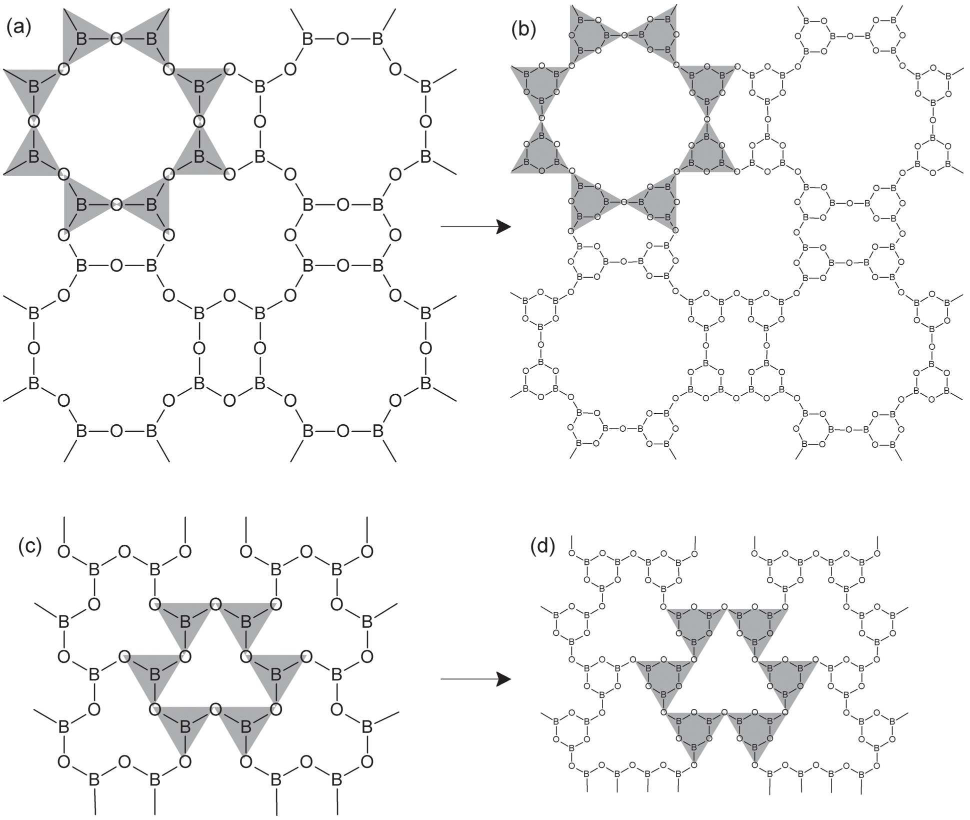

Figure 2. Equivalent 2D sheets consisting of a,c) BO_3 units and b,d) B_3O_3-rings. The replacement of each boron atom with a B_3O_3 ring preserves the connectivity and the stoichiometry; (a) generates (b), and (c) generates (d). The sheets in (a,b) contain nanopores surrounded by 4, 6, and 8 building blocks and were used to construct Structures C and C-R. In the sheets in (c,d) all nanopores are surrounded by 6 building blocks (shown in grey); this sheet was used to construct Structures D and D-R.

B_3O_3) once again connected by B-O-B bridges (Structure F in Figure 3 in ref. [18]) to form a 3D-network. **Figure 5** shows the energy variation of this structure with volume. Again this is remarkably flat, varying by < 5 kJ mol^{-1} over the volume range 12–30 Å^3 $atom^{-1}$, even if not as broad as for the B_2O_3 structures containing B_3O_3 rings (Figure 4).

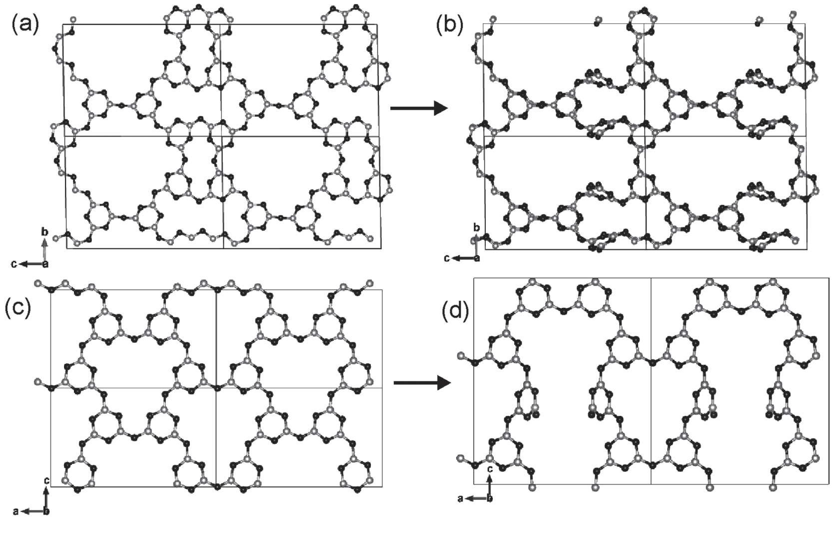

Figure 3. a) 2D sheet used to generate b) 3D Structure C-R; c) 2D sheet used to generate d) 3D Structure D-R. Boron atoms are grey and oxygen atoms are black.

3. Discussion

In order to probe the remarkable energy variation, we have examined the structures of the ultra-flexible forms at different volumes. Bond lengths hardly change. For example, for Structure D-R, at a volume of 12 Å^3 $atom^{-1}$, the B-O bond lengths are between 1.35 and 1.39 Å, while at a volume of 78 Å^3 $atom^{-1}$ the bond lengths are between 1.38 and 1.43 Å. These are similar in Structure C-R. In contrast, again looking at structure D-R, at the smaller volume the B-O-B bridge angles are between 123° and 143°, while at the larger volume they lie between 165° and 180°—a very large variation. Again C-R is similar. The intra-ring angles hardly change and are always close to 120°. This suggests that one primary cause of the very broad energy vs. volume curve is the flexibility of the B-O-B bridging bonds.

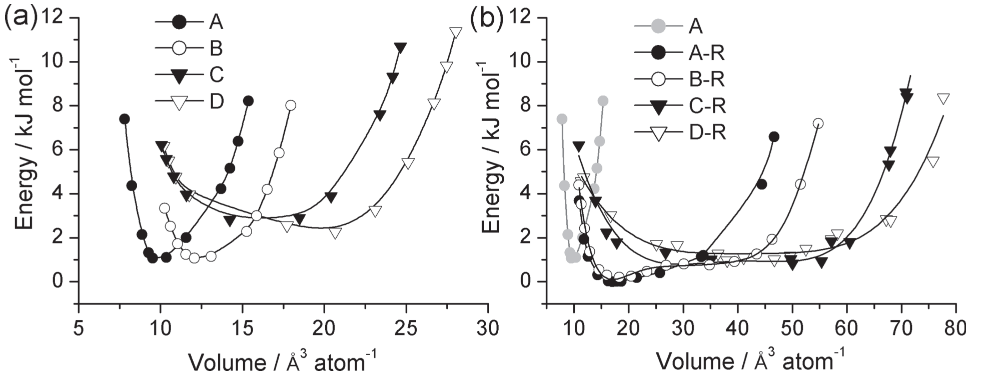

Figure 4. Energy (per mole of atoms) vs. volume curves for a) the four structures without B_3O_3 rings A-D and b) their analogues with B_3O_3 rings, A-R, B-R, C-R, D-R. All energies are plotted relative to the lowest energy calculated, the minimum for Structure A-R. Structure A is included in both plots for comparison. The interconnecting lines are fourth order polynomial fits present solely to guide the eye.

Similarly, for BO, at small volume the bond lengths are almost identical to those at much larger volumes; the changes in the structure at different volumes are reflected in the bridging B-O-B angles and accompanying changes in the torsion angles which govern the relative orientation of neighboring rings.

As the unit cell size increases from A/A-R to D/D-R, the flexibility of the structure (i.e., the width of the minimum in the energy vs. volume plot) increases. For example, structures C/C-R and D/D-R were built from 2D sheets, and the volume of the primitive unit cell is larger for D/D-R. Both contain two intersheet connections per cell, so the flexibility appears to be associated with the density of these interlayer connections. A/A-R and B/B-R have smaller unit cells and are more interlocked structures; they are clearly less flexible than C/C-R and D/D-R.

The energy–volume curves in Figure 4 show that the B_2O_3 structures without the B_3O_3 rings (A to D, Figure 4a) are much denser and topologically more rigid than those with these rings (A-R to D-R, Figure 4b); the energy minima are much narrower. Very large B-O-B angles are more readily accessible to structures with these rings. For example in Structure A, the B-O-B bond angles at an energy of 10 kJ mol^{-1} above the minimum (on the high-volume side) are between 150° and 166°, while for comparison in A-R the bridging B-O-B angles are all 180°. For Structure D at the same energy, the B-O-B bond angles vary from 158° to 180° (with 16 of 24 angles in the unit cell < 160°), while for D-R the bridging angles lie between 165° and 180°. Thus the overall flexibility of the structures appears to be related in part to the flexibility of these B-O-B angles in structures containing rings. Structures D and A-R have approximately the same optimized unit cell volume but A-R is much more flexible (Figure 5), suggesting that the flexibility is not simply an effect of the unit cell size. A difference in the flexibility of the O-B-O angles in the structures with and without rings may also play a role; at an energy of 10 kJ mol^{-1} above the minimum, in Structure D-R, these angles vary between 114.5° and 123.6°, compared with a range of only 118.6° to 120.7° in Structure D.

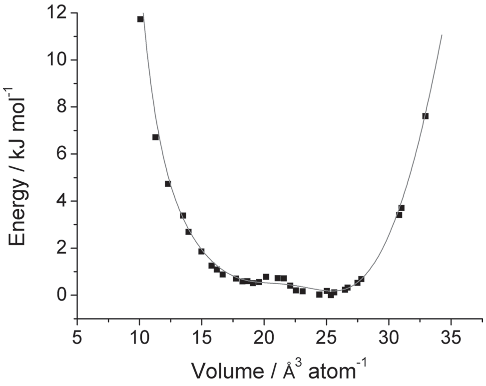

Figure 5. Energy (per mole of atoms) vs. volume for boron monoxide (Structure F from ref. [18]). The interconnecting line is a fourth order polynomial fit present solely to guide the eye.

In this context and with reference to Figure 2, it is worth noting that in structures containing B_3O_3 rings the formation of the low-density structure requires each boron to participate in one near-linear B-O-B linkage. The remaining two B-O-B linkages which form part of the B_3O_3 ring remain bent. In contrast when B_3O_3 rings are absent every boron atom participates in three near-linear B-O-B links; this arrangement appears to correspond to a much higher energy penalty for increasing the B-O-B bond angle. This is consistent with the formal valence bond picture presented in Scheme 1; the first-row element boron is restricted to an octet of outer shell electrons. This suggests that it is the flexibility of B-O-B bonds, as observed in small molecules, in conjunction with particular structural features in the solid state that produces these remarkably flat energy vs. volume curves.

Across different silicates, considerable variations in Si-O-Si angle are seen, consistent with the flexibility observed in analogous molecules, but individual solid silicates do not possess energy vs. volume curves with such wide minima as those presented here. Silicon is four coordinate rather than three, and while individual Si-O-Si linkages can be flexible, such as those connecting corner-sharing tetrahedra, it appears that there is a significant energy penalty when a single Si is associated with more than one large bond angle. More work remains to be carried out on the importance of other structural features in determining flexibility more generally.

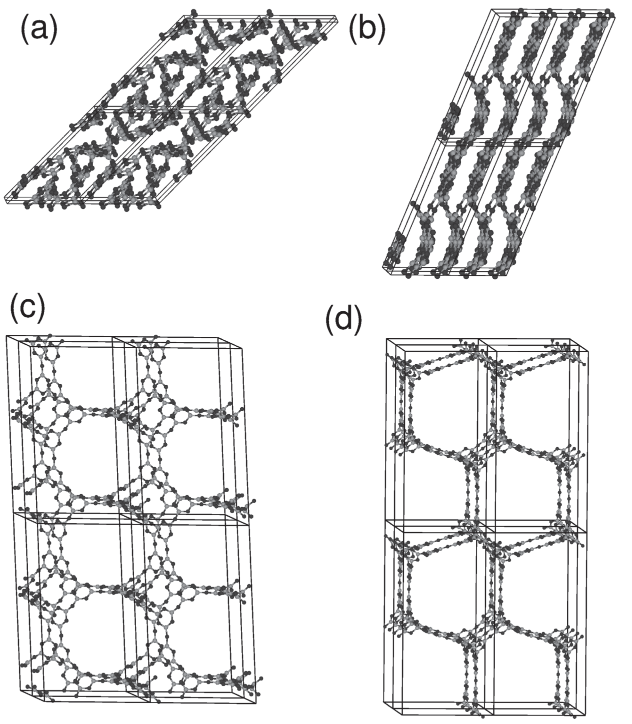

Figure 6. The structures adopted by C-R and D-R at representative low and high volumes (10 and 70 Å^3 atom^{-1}, respectively): a) C-R at low volume; b) D-R at low volume; c) C-R at high volume; d) D-R at high volume. Boron atoms are grey and oxygen atoms are black.

On the high-volume side of the energy minima, the structures are nanoporous. The overall effect of the volume change is a collapse of the nanopores at small volume. The structures adopted by C-R and D-R are shown for representative high and low volumes (10 and 70 Å^3 atom^{-1} respectively) in **Figure 6**. Similar behavior is seen for the BO structure (shown in the Supporting Information).

It is important to note that all the structures investigated are low in energy and so thermodynamically accessible. Each structure with a B_3O_3 ring is very similar in energy to its analogue without the ring and all of the structures containing such rings have very similar energies to Structure A, the known α-B_2O_3 crystal structure. Our results also predict the instability of structures with B_3O_3 rings relative to those without at very low volumes (high pressures).

The inability to find structural models with the experimental density for vitreous B_2O_3 (1.8 g cm^{-3}) and in which most of the boron atoms are in B_3O_3 rings has been a long-standing and controversial aspect of B_2O_3 structure prediction and analysis.[12,24,25] The ultra-flexibility of the structures with B_3O_3 rings provides a resolution to this problem since a small variation in the B-O-B angles in the bridges in structures with B_3O_3 rings has a large effect on the volume and thus also on the density. But the energetic cost of this volume variation is negligible. Our results also confirm the higher relative stability of structures with B_3O_3-rings at larger volumes and thus typical glass densities. Previous studies relying on empirical force-fields with harmonic angular B-O-B terms are likely to be inaccurate because they cannot reproduce the energy variation of the polymorphs with B_3O_3 rings which our quantum mechanical calculations have revealed.

4. Conclusion

Overall we have demonstrated the stability and energetic feasibility of boron oxide structures that are stable over a very wide volume range. The striking flexibility in B-O-B bond angles, unusual for covalent bonds and evident in both 3D structures and small molecular analogues, leads to an unprecedented wide range of possible densities. The energy variation with volume of 3D structures in which six-membered B_3O_3 or B_4O_2 rings are linked by single B-O-B bridges is minimal over a wide range of volumes; there are very broad minima in the potential energy surface, with equienergetic configurations differing in volume by well over a factor of two. All our calculated structures are low in energy. Low-density frameworks have been reported or predicted for other materials,[6–8] but in such cases in marked contrast these low-density phases are considerably higher in energy then the denser polymorph. As a result of the ability to modify the B-O-B bridging angle with negligible change in energy, 3D structures containing these bonds are ultra-flexible. At their volume maximum, these boron oxide structures are nanoporous with very low density; the pores can be readily collapsed and expanded. These materials thus offer in principle a wide range of structural, and thus chemical and electronic, possibilities, as well as novel guest-host systems. The flexibility of these structures also offers a resolution of the long-standing controversy regarding the structure and density of vitreous B_2O_3. Successful synthesis of these nanoporous materials may well require methods which promote formation of low-density structures such as template-directed techniques. We hope this study will encourage experimental efforts towards the synthesis and characterization of these materials with such unusual energy profiles.

5. Methods

Molecular calculations were carried out with the Jaguar program,[26] using the hybrid Becke three-parameter exchange functional,[27] the Lee-Yang-Parr correlation functional[28] (B3LYP), and the 6-31G** basis set. CASSCF calculations were also carried out on H_2B-O-BH_2 to confirm that a single determinant description is sufficient for this type of molecule and confirm the MP2 and MP4 results for this molecule.

For the solid-state materials, we carried out periodic ab initio calculations using plane-wave density functional theory (DFT) calculations in the generalized gradient approximation (GGA) as implemented in the CASTEP code[29] with the Perdew-Wang exchange correlation functional.[30] Only valence electrons were considered, with core electrons replaced by default on-the-fly pseudopotentials. After consideration of the energy cut-off for the plane waves (given in Supporting Information), a cut-off of 490 eV was selected. Reciprocal space integration utilized the Monkhorst-Pack sampling scheme[31] and convergence of the energy with the number of *k*-points was checked carefully. For fixed cell volume calculations, all cell parameters and atomic positions were optimized by energy minimization using a conjugate-gradient algorithm with maximum force tolerance 0.01 eV Å^{-1}, an energy convergence criterion of 5×10^{-6} eV, and a displacement convergence criterion of 1×10^{-3} eV. There were no symmetry constraints. Calculated unit cell parameters and bulk modulus for the experimentally known B_2O_3 structures, given in the Supporting Information, are in good agreement with experiment with differences those typically observed in GGA calculations. Additionally, the structural parameters of and the energy difference between the A and A-R structures obtained by PW91/GGA calculations were in good agreement with calculations using different exchange correlation functionals (PBE) and calculations at different levels of theory (LDA and B3LYP). These results are given in the Supporting Information.

Supporting Information

Supporting Information is available from the Wiley Online Library or from the author.

Acknowledgements

The authors thank Chris Russell and Fred Manby for fruitful discussion.

Received: January 15, 2013
Revised: March 28, 2013

[1] K. Doll, J. C. Schön, M. Jansen, *Phys. Chem. Chem. Phys.* **2007**, *46*, 6128.
[2] J. C. Schön, K. Doll, M. Jansen, *Phys. State. Solidi B* **2010**, *247*, 23.
[3] C. E. Sims, G. D. Barrera, N. L. Allan, W. C. Mackrodt, *Phys. Rev. B* **1998**, *57*, 11164.
[4] C. L. Freeman, F. Claeyssens, N. L. Allan, J. H. Harding, *Phys. Rev. Lett.* **2006**, *96*, 066012.
[5] C. Tusche, H. L. Meyerheim, J. Kirschner, *Phys. Rev. Lett.* **2007**, *99*, 026102.
[6] J. Carrasco, F. Illas, S. T. Bromley, *Phys. Rev. Lett.* **2007**, *99*, 235502.
[7] M. A. Zwijnenburg, S. T. Bromley, *Phys. Rev. B* **2011**, *83*, 024104.
[8] M. A. Zwijnenburg, S. T. Bromley, *J. Mat. Chem.* **2011**, *21*, 15255.
[9] W. Sangthong, J. Limtrakul, F. Illas, S. T. Bromley, *J. Mater. Chem.* **2008**, *18*, 5871.
[10] H. Hubert, B. Devouard, L. A. J. Garvie, M. O'Keeffe, P. R. Buseck, W. T. Petuskey, P. F. McMillan, *Nature* **1998**, *391*, 376.
[11] L. Huang, J. Kieffer, *Phys. Rev. B* **2006**, *74*, 224107.
[12] G. Ferlat, A. P. Seitsonen, M. Lazzeri, F. Mauri, *Nat. Mater.* **2012**, *11*, 925.
[13] N. Umesaki, Y. Kita, T. Kirihara, T. Iida, T. Fukunaga, M. Misawa, *J. Non-Cryst. Solids* **1994**, *177*, 200.
[14] F. Gatti, N. Berthe-Gaujac, I. Demachy, F. Volatron, *Chem. Phys. Lett.* **1995**, *232*, 503.
[15] G. V. Gibbs, *Am. Mineral.* **1982**, *67*, 421.
[16] M. O'Keeffe, P. F. McMillan, *J. Phys. Chem.* **1986**, *90*, 541.
[17] G. V. Gibbs, M. B. Boisen, F. C. Hill, O. Tamada, R. T. Downs, *Phys. Chem. Miner.* **1998**, *25*, 574.
[18] A. Navrotsky, K. L. Geisinger, P. McMillan, G. V. Gibbs, *Phys. Chem. Miner.* **1985**, *11*, 284.
[19] I. Petrovic, A. Navrotsky, M. E. Davis, S. I. Zones, *Chem. Mater.* **1993**, *5*, 1805.
[20] G. E. Gurr, P. W. Montgomery, C. D. Knutson, B. T. Gorres, *Acta Cryst.* **1970**, *B26*, 906.
[21] M.-S. Wang, G.-C. Guo, W.-T. Chen, G. Xu, W.-W. Zhou, K.-J. Wu, J.-S. Huang, *Angew. Chem. Int. Ed.* **2007**, *46*, 3909.
[22] M.-C. Liu, P. Zhou, H.-G. Yao, S.-H. Ji, R.-C. Zhang, M. Ji, Y.-L. An, *Eur. J. Inorg. Chem.* **2009**, *31*, 4622.
[23] F. Claeyssens, N. L. Allan, N. C. Norman, C. A. Russell, *Phys. Rev. B* **2010**, *82*, 094119.
[24] G. Ferlat, T. Charpentier, A. P. Seitsonen, A. Takada, M. Lazzeri, L. Cormier, G. Calas, F. Mauri, *Phys. Rev. Lett.* **2008**, *101*, 065504.
[25] R. J. Bell, A. Carnevale, *Phil. Mag. B* **1982**, *43*, 389.
[26] Jaguar version 5.5, Schrödinger, L.L.C. (Portland, OR, 1991-2003).
[27] A. D. Becke, *J. Chem. Phys.* **1993**, *98*, 5648.
[28] C. T. Lee, W. T. Yang, R. G. Parr, *Phys. Rev. B* **1988**, *37*, 785.
[29] S. J. Clark, M. D. Segall, C. J. Pickard, P. J. Hasnip, M. I. J. Probert, K. Refson, M. C. Payne, *Z. Kristall.* **2005**, *220*, 567.
[30] J. P. Perdew, Y. Wang, *Phys. Rev. B* **1992**, *45*, 13244.
[31] H. J. Monkhorst, J. D. Pack, *Phys. Rev. B* **1976**, *13*, 5188.